Investigation of Matter Effects in Neutrino Oscillations with IceCube Sensitivity

DESY Summer Student Programme, 2012

A. M. W. Mitchell

University of Warwick, Coventry, UK, CV4 7AL

Supervisors:
R. Nahnhauer, J. P. Yanez

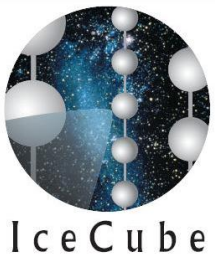

31st of August 2012

Abstract

Matter effects modify the oscillation probabilities of atmospheric neutrinos when compared to their vacuum values. A step function density profile for the Earth is used to investigate these matter effects for both normal and inverted neutrino mass hierarchy schemes. From a realistic simulation, the oscillation probabilities as a function of energy and zenith angle are shown, comparing matter and vacuum cases. Detector restrictions specific to IceCube are then imposed, with an preliminary indication of whether the neutrino mass hierarchy can be determined.

THE UNIVERSITY OF WARWICK

DESY

Contents

1 Introduction

As neutrinos propagate freely through space they undergo flavour changing oscillations. When travelling through matter, the rate and amplitude of these oscillations are modified in a manner dependant on the electron density. Experimental measurements of these matter effects is desirable in order to obtain further details and constraints on the nature of the elusive neutrinos. Alternatively, for a well understood neutrino source these measurements may provide information about the matter it has passed through. This report focusses on atmospheric neutrinos and their detection by the IceCube experiment.

IceCube is a neutrino observatory situated at a depth of between 1.5km and 2.5km within the Antarctic ice [1]. At this depth, few photons from the surface can penetrate and the ice is remarkable clear. The detector comprises a total of 5160 digital optical modules (DOMs), each of which is equipped with a Photo Multiplier Tube, connected to cables buried vertically in the ice. DeepCore is a region at the heart of the IceCube array in which the DOMs are positioned closer together; and hence is optimised for low energies (down to $\sim$ 10GeV). The neutrinos detected by IceCube may originate from three main sources: from atmospheric cosmic ray showers, from astrophysical sources and from the decay of hypothetical dark matter particles.

Atmospheric neutrinos are produced by cosmic ray showers in the Earth's atmosphere, at an average height of around 15km [2]. They encompass a wide energy range from MeV to PeV, with a peak flux at a few GeV [3]. Various models estimating the flux of atmospheric neutrinos are available; in this project the Honda flux model is used [4].

At the energies to which IceCube is sensitive ($10\text{GeV} - 10^9\text{GeV}$), the primary type of neutrino interaction with matter is Deep Inelastic Scattering (DIS), which may be either charged current, $\nu_l + N \rightarrow l + X$ in which the lepton corresponding to the neutrino flavour is produced; or neutral current, $\nu_l + N \rightarrow \nu_l + X$ in which the neutrino remains, but a hadronic cascade is also triggered. The particles released by these interactions have sufficient energy to travel faster than the local speed of light, thus emitting Cherenkov radiation, which is detected by the DOMs as an 'event'. The signatures of these events fall into two main classes of track-like and cascade-like according to the dominant feature, which also varies with neutrino type. Track-like events produced by muon neutrinos in charged current interactions are used for this study [1].

As the effect of neutrino oscillations is enhanced over longer baselines and lower energies (see section 2), in this project we are concerned with upwards travelling (zenith angle $90^\circ \leq \theta_z \leq 180^\circ$) muon neutrino events in DeepCore. This ensures that the neutrino trajectories have passed through a significant amount of matter, namely the Earth, prior to detection. Therefore, in simulating the influence of matter effects on neutrino oscillations, we consider a density profile suitable for the Earth prior to adding detector effects specific to IceCube.

In this report, a brief theoretical overview of neutrino oscillations and matter effects is given in section 2. The algorithm used is described in section 2.3, with some illustrative plots of the consequences of matter on neutrino oscillation probabilities. Incorporation of various detector performance features specific to IceCube is outlined in section 3 and followed with some preliminary indications regarding the effects detectability. We then conclude in section 4, mentioning the direction of further work.

2 Theory

2.1 Neutrino Oscillations in Vacuum

A fundamental property of neutrinos is that their familiar flavour states do not directly correspond to mass eigenstates, but to a superposition of massive neutrino states. This may be accounted for by converting between mass and flavour neutrino states where necessary by the use of a mixing matrix, U. A flavour state is then given by $|\Psi_\alpha\rangle = \sum_{k=1}^{3} U^*_{\alpha k}|\Psi_k\rangle$, where the indices k and α refer to the mass and flavour eigenstates respectively. U is completely defined by a set of four terms; three real and one imaginary. The most common formulation of U comprises terms dependent on real mixing angles between the mass eigenstates; θ_{13}, θ_{23} and θ_{12}; and also on an imaginary phase, δ_{CP}. The form of U is: (using $\sin\theta_{12} = s_{12}$ and $\cos\theta_{12} = c_{12}$ etc.)

$$U = \begin{pmatrix} c_{12}c_{13} & s_{12}c_{13} & s_{13}e^{-i\delta_{CP}} \\ -s_{12}c_{23} - c_{12}s_{23}s_{13}e^{i\delta_{CP}} & c_{12}c_{23} - s_{12}s_{23}s_{13}e^{i\delta_{CP}} & s_{23}c_{13} \\ s_{12}s_{23} - c_{12}c_{23}s_{13}e^{i\delta_{CP}} & -c_{12}s_{23} - s_{12}c_{23}s_{13}e^{i\delta_{CP}} & c_{23}c_{13} \end{pmatrix}. \quad (1)$$

Particle evolution through space and time is described quantum mechanically by the Schrödinger equation; which requires a particle description as energy, or equivalently mass, eigenstates. The solution to the Schrödinger equation in the case of neutrinos is the evolution matrix operator:

$$M = diag\left(1, \exp\left(\frac{-i\Delta m^2_{21}L}{2E}\right), \exp\left(\frac{-i\Delta m^2_{31}L}{2E}\right)\right), \quad (2)$$

where $\Delta m^2_{21} = m^2_2 - m^2_1$ and $\Delta m^2_{31} = m^2_3 - m^2_1$ are the squared mass differences, L is the distance travelled and E the neutrino energy. The flavour amplitude of the neutrino oscillation state is therefore given by:

$$|\Psi_\alpha\rangle = UMU^*|\Psi_\alpha\rangle, \quad (3)$$

and the probability of a neutrino being detected with a particular flavour after travelling is obtained from the square of the amplitude in equation (3).

For the simplified case of two flavour neutrino oscillations,[1] there is only one mixing angle θ and one mass difference Δm^2, such that the probability of flavour change is simply given by:

$$P_{\nu_\alpha \to \nu_\beta} = \sin^2(2\theta)\sin^2\left(\frac{\Delta m^2 L}{4E}\right). \quad (4)$$

Here the first term is dependent on the mixing angle and determines the amplitude of the oscillation, whilst the second term is a phase term. As can be seen from the dependence on L/E, the oscillation probability is enhanced over longer distances and lower energies. If L/E varies too slowly, the $\sin$ terms in which it features go to zero, whereas if L/E varies too quickly (i.e. $L \gg L_{osc} = \frac{4\pi E}{\Delta m^2}$, the oscillation length) the terms are averaged out.

As the final state amplitude in equation (3) is a vector, the probability of each flavour individually is obtained from the appropriate element. The final expression for the probability consists of terms of the form of those appearing in equation (4).

[1] For the sake of brevity, the standard derivation of the oscillation probability in a vacuum case is not reproduced here; see for example [5].

The current best experimental values for the mixing angles and squared mass differences are given in table 1. Note that all of the mixing angles have non-zero values, and that between the mass squared differences:

$$\Delta m^2_{21} \ll \Delta m^2_{31} \simeq \Delta m^2_{32}. \qquad (5)$$

Parameter	Experimental Value
Δm^2_{21}	$7.59^{0.20}_{0.18} \times 10^{-5}\text{eV}^2$
$\lvert\Delta m^2_{31}\rvert$	$2.34^{+0.1}_{0.09} \times 10^{-3}\text{eV}^2$
$\sin^2(2\theta_{12})$	$0.312^{+0.017}_{-0.015}$
$\sin^2\theta_{23}$	0.51 ± 0.06
$\sin^2\theta_{13}$	$0.089 \pm 0.01(\text{stat.}) \pm 0.005(\text{syst.})$
δ_{CP}	Unknown

Table 1: Parameter values used in this project, from most recent experimental results as of July 2012 [6]

As no experiment yet has been able to distinguish between $\Delta m^2_{31} \simeq \Delta m^2_{32}$, they are set to the same value, denoted $|\Delta m^2_{31}|$. Atmospheric neutrino experiments are only sensitive to one of these mass differences, whilst solar neutrino experiments are only sensitive to the other. Therefore, Δm^2_{21} and $|\Delta m^2_{31}|$ are termed the solar and atmospheric mass squared differences respectively.

The relation between the masses in (5) may be accommodated into two different neutrino schemes, termed normal and inverted hierarchy, as shown in figure 1. At this point in time, the nature of the neutrino mass hierarchy as normal or inverted is not determined. As can be seen from figure 1, a change in hierarchy corresponds to a change in the sign of Δm^2_{31}.[2]

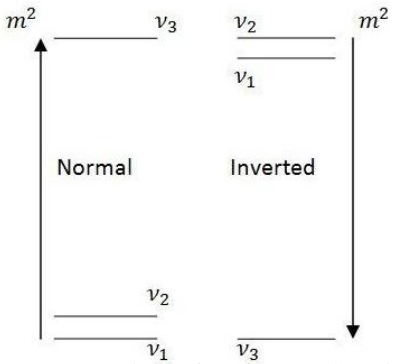

Figure 1: Schematic of normal and inverted mass hierarchies

2.2 Matter Effects in Neutrino Oscillations

When neutrinos travel through matter, the Hamiltonian in the Schrödinger equation becomes modified by the addition of an extra potential term which depends on the Fermi constant, G_F and the electron number density, $N_e(x)$:

$$V(x) = \sqrt{2} G_F N_e(x), \qquad (6)$$

which comprises an arbitrary density profile. The matter modified Hamiltonian is $H = \frac{1}{2E}(UMU^* + A)$, where A is a matrix with only one element; $A = diag(A_{CC}, 0, 0)$, and $A_{CC} = 2EV(x)$, the CC subscript emphasising that charged current interactions are under consideration. In the case of a constant matter density profile $N_e(x) = N_e$, the mass squared differences and mixing angles take on effective values within the medium. The effective value of Δm^2_{31} in matter is given by:

$$\Delta m^2_{M31} = \sqrt{(\Delta m^2_{31}\cos 2\theta_{13} - A_{CC})^2 + (\Delta m^2_{31}\sin 2\theta_{13})^2} \qquad (7)$$

and the effective value of θ_{13} is given by:

$$\cos 2\theta_{M13} = \frac{\Delta m^2_{31}\cos 2\theta_{13} - A_{CC}}{\Delta m^2_{M31}}, \sin 2\theta_{M13} = \frac{\Delta m^2_{31}\sin 2\theta_{13}}{\Delta m^2_{M31}}. \qquad (8)$$

It is perhaps illustrative to consider the tangent expression obtained by equations (8);

$$\tan 2\theta_{M13} = \frac{\tan 2\theta_{13}}{1 - \frac{A_{CC}}{\Delta m^2_{31}\cos 2\theta_{13}}}, \qquad (9)$$

[2]Note also that in figure 1 the order of ν_1 and ν_2 does not change; this has been fixed by solar neutrino experiments, as the neutrino with the highest ν_e content is the lightest [5].

from which it can be seen that there is a resonance when $A_{CC} = \Delta m^2_{31} \cos 2\theta_{13}$; then $\theta_{M13} = \frac{\pi}{4}$, at which point the mixing is maximal and hence the transition probability is also maximised. In calculating the matter modified mixing angle, the cosine expression in equation (8) is used to provide the correct phase. For atmospheric neutrinos, only θ_{13} is modified, θ_{23} retaining the vacuum value and the mixing matrix (equation (1)) becomes:[3]

$$U_M = \begin{pmatrix} c^M_{13} & 0 & s^M_{13} e^{-i\delta_{CP}} \\ -s_{23} s^M_{13} e^{i\delta_{CP}} & c_{23} & s_{23} c^M_{13} \\ -c_{23} s^M_{13} e^{i\delta_{CP}} & -s_{23} & c_{23} c^M_{13} \end{pmatrix}. \quad (10)$$

It should be noted that equations (7) and (8) include a dependence on the sign of Δm^2_{31}. With experiments sensitive to matter effects it may be possible to distinguish between the different values of Δm^2_{M31} expected to result from the hierarchy schemes in figure 1, thereby determining which of the two hierarchies is correct.

2.3 Matter Effects due to the Earth's density profile

Up until now only the case of constant electron density has been discussed, whilst the atmospheric neutrinos reaching the detector actually cross the Earth. Although the Earth's density is not constant, various density profiles may be used to describe it, such as parabolic, $\frac{1}{x}$, polynomial, etc. (see [7], [8]). The simplest approximation for the density (which has been widely used [2, 12, 14]) is as a series of constant density layers. To obtain the state amplitude for a neutrino trajectory which traverses multiple (n) layers, equation (3) must be applied successively through each layer [5]:

$$|\Psi_\alpha\rangle = [U_M M(x_n - x_{n-1}) U^*_M]_n \ldots [U_M M(x_2 - x_1) U^*_M]_2 [U_M M(x_1 - x_0) U^*_M]_1 |\Psi_\alpha\rangle, \quad (11)$$

where the distance travelled in layer n, $x_n - x_{n-1} = L_n$ is used in equation (2). As the density changes through different media, so the potential and hence the effective values of θ_{M13} and Δm^2_{M31} will also change, as shown in equations (7) and (8). Comparison with the Preliminary Reference Earth Model (PREM) shows that the approximation is reasonable; to a first approximation, a two layer step function of core and mantle only may be used (see figure 2) [9, 5]. Equation (11) is used with $n = 1$ or 3, depending on whether or not a neutrino crosses the core. Distinguishing between mantle-core-mantle and mantle-only trajectories is possible given the direction of the neutrino. Those neutrinos with a zenith angle less than $\theta_z = 146.83°$ do not traverse the core[4], as shown in figure 2.

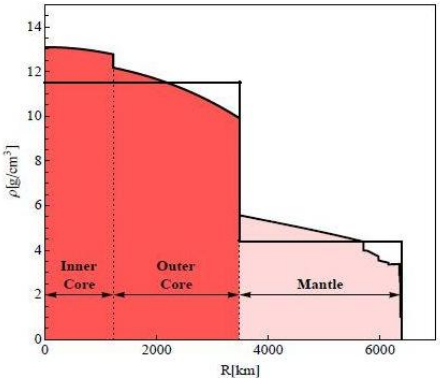

Figure 2: The PREM model as approximated with a simplistic mantle-core-mantle step function. Adapted from [10].

In this work, the above matrix formulation was used in calculating the expected flavour probabilities as a function of baseline length L (i.e. direction) and as a function of energy. By imposing

[3] When considering atmospheric neutrinos, the effects due to the solar components are not detectable, and the parameters Δm^2_{21} and θ_{21} may be set to zero. Conversely, in solar neutrino experiments the terms due to the atmospheric components are averaged out.

[4] This critical angle is obtained from the geometry of the Earth; trajectories with a zenith angle greater than $180° - \sin^{-1}\left(\frac{R_c}{R_\oplus}\right)$, where R_c and $R_\oplus$ are the mean radii of the core and Earth respectively, do not traverse the core [11].

a check to determine whether a given direction corresponds to a core-crossing trajectory, and subsequently looping over the number of layers, the following plots were produced.

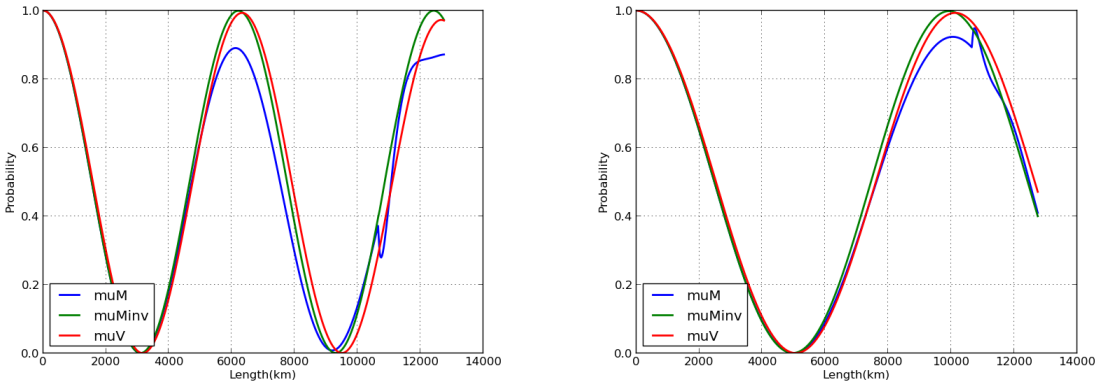

Figure 3: Muon neutrino flavour probability against baseline through the Earth for vacuum (V) and matter (M) cases with both normal and inverse (inv) hierarchies, at (left) 5GeV and (right) 8GeV. The deviation from the vacuum case due to matter effects for the normal hierarchy is greater than for inverse hierarchy. The effect of the mantle-core boundary is noticeable at 10,665km. The deviation of matter effects from the vacuum case, whilst pronounced at 5GeV, have decreased significantly by 8GeV.

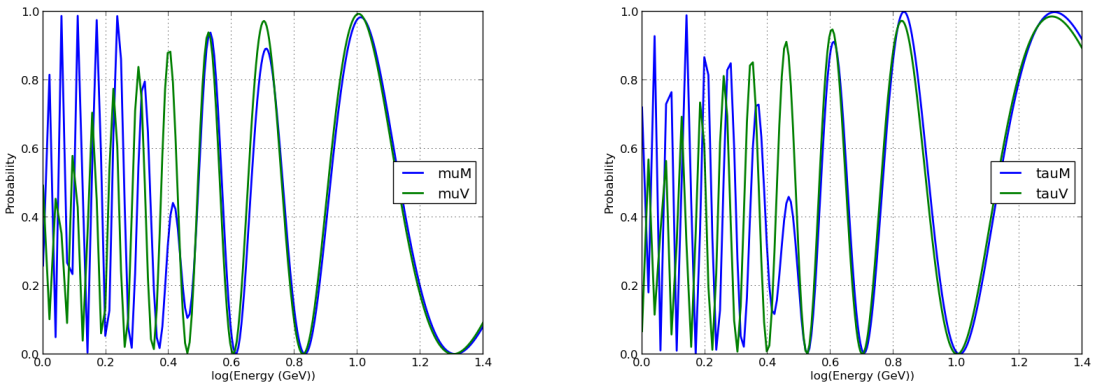

Figure 4: Flavour probability for muon (left) and tau (right) neutrinos as a function of neutrino energy using the diameter of the Earth as a baseline (zenith angle of π), in vacuum (V) and matter (M) cases. Both plots use normal mass hierarchy, and are in agreement with [12], the deviation due to matter effects decreasing with increasing energy.

Figure 3 shows the oscillation probability as a function of length for an initial muon neutrino. As the matter effects are more pronounced in the case of normal hierarchy, in figure 4 the probability is shown as a function of the neutrino energy for normal hierarchy only, again for an initial muon neutrino. Here it can be seen that the oscillation probabilities only deviate appreciably from the vacuum case at low energies; beyond about 25GeV the effects are washed out. Comparison of figure 4 with [13] shows that this is indeed the expected behaviour with the Earth as a baseline. The survival probability of

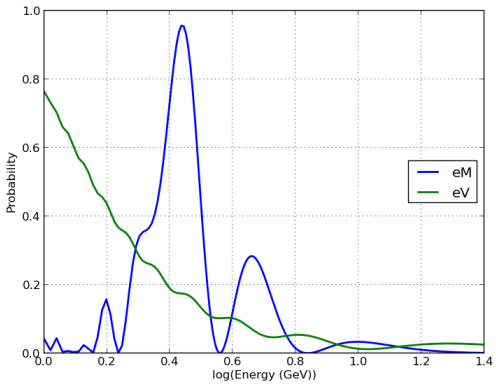

Figure 5: Electron neutrino probability as a function of energy for normal mass hierarchy and an initial electron neutrino, in agreement with [14].

electron neutrinos in particular, figure 5, is in agreement with the result presented by [14], also using the Earth's diameter as a baseline.

3 Matter Effects in Detection of Atmospheric Neutrino Oscillations

3.1 General neutrino interaction rate

To address the likelihood of the detection of matter effects in atmospheric neutrino experiments, firstly the case of a general atmospheric neutrino interaction rate is addressed. This would hold true in the vicinity of any neutrino detector, as no detector specific effects were added at this stage in the simulation. The Honda atmospheric flux was used to provide a suitable initial neutrino rate, and the GENIE[5] neutrino simulator provided realistic details of neutrino interaction kinematics [4, 15]. Based on information from the simulation, the code implemented distinguishes whether the trajectory is core-crossing or not, and calculates the state amplitude using equation (11). The final probability is a vector comprising the probabilities for each neutrino flavour. The equivalent probabilities for the vacuum (same energy and baseline) and no oscillation cases are also calculated. In all plots within this section of the report, δ_{CP} is set to zero and the neutrino flux that could be expected in one cubic kilometre after one year was used [16].

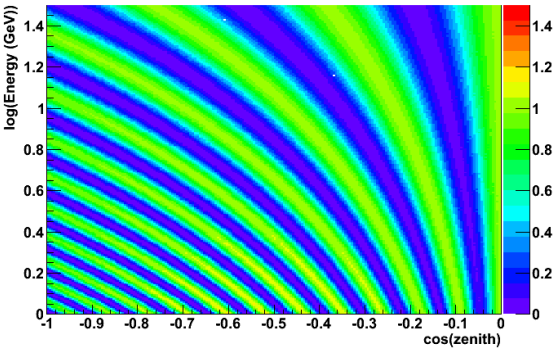

Figure 6: Neutrino oscillogram showing the ratio of vacuum to no oscillation survival probabilities for muon neutrino/anti-neutrino events combined with energy and zenith angle.

Neutrino oscillograms show the ratio of muon neutrino and anti-neutrino events combined to the no oscillation case for a given energy and zenith angle. In figure 6 the vacuum case is presented, which is unaffected by the hierarchy change (see section 2.2). The oscillograms showing the ratio of the matter effects to no oscillation case are depicted in figure 7 for both cases of normal mass hierarchy and inverse hierarchy, in agreement with the results in [17].

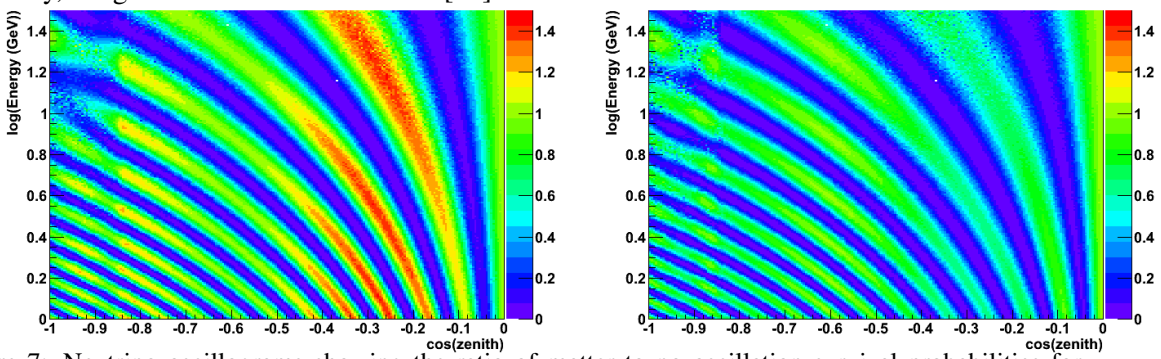

Figure 7: Neutrino oscillograms showing the ratio of matter to no oscillation survival probabilities for muon neutrino/anti-neutrino events combined, as a function of energy and zenith angle. The left plot is for normal and the right for inverse mass hierarchies. The mantle-core boundary is seen as a feature occurring at cos(zenith)=0.84.

The probability ratio scale may be seen to rise slightly above one; as the initial neutrino flux is mixed, this is due to the additional contribution to the muon neutrino total by the oscillation

[5] Generates Events for Neutrino Interaction Experiments

of electron neutrinos into muon neutrinos. The ratio between these vacuum and matter cases is shown in figure 8, with the high ratio in some bins due to a change in phase between the two cases causing division by a small number of events to occur. It is more instructive to consider the integrated number of events, shown in figures 9 and 10. In all of figures 6-8, the energy scale is limited to below approximately 25GeV, since the influence of matter effects was shown to be negligible at higher energies (see section 2.3).

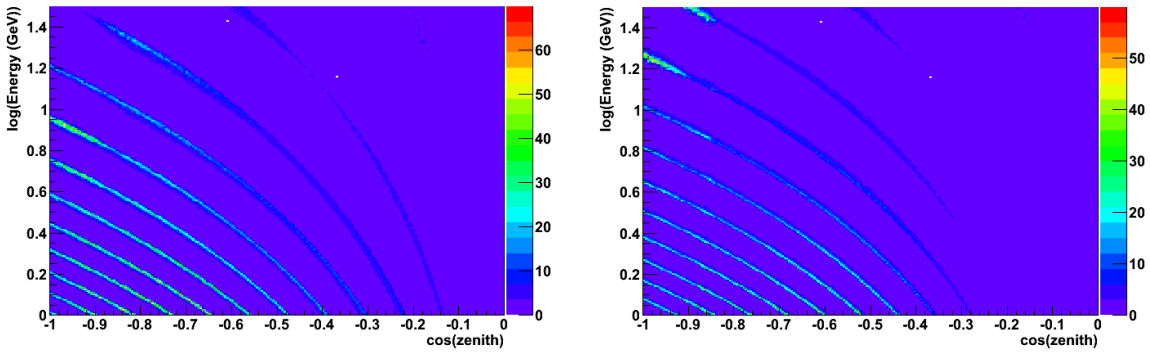

Figure 8: Ratio of matter to vacuum oscillations: left in the case of normal mass hierarchy; right in the case of inverted mass hierarchy.

The number of neutrino events expected in the three cases; no oscillations, vacuum oscillations and addition of matter effects; varies between them due to the different probabilities. This variation is depicted in figures 9 and 10, alongside the ratio of the vacuum and matter cases to no oscillations, which drops below one as the difference in the probabilities becomes significant (towards longer baselines and lower energies, section 2.1). Due to a recently discovered issue with the flux calculation in IceCube, simulation events with energies lower than 8GeV were cut from figure 10, similarly figure 9 is shown for the energy range of interest, $8 - 25$GeV.

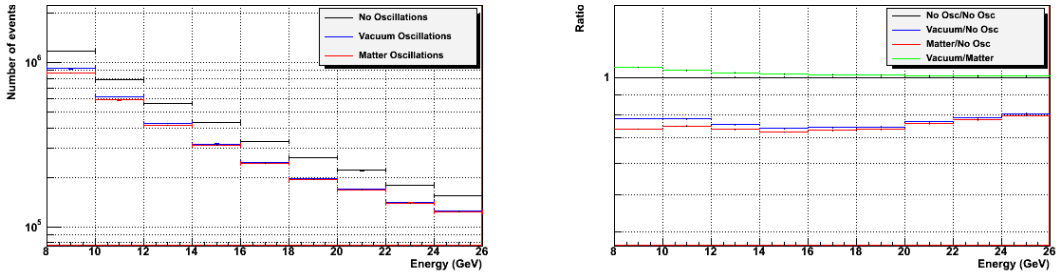

Figure 9: The number of muon neutrino events can be seen to deviate between oscillation and no oscillation cases at low energy. Whilst the difference between matter and vacuum cases is far from obvious, it can be seen in the deviation of the green line from one at low energies in the ratio plot.

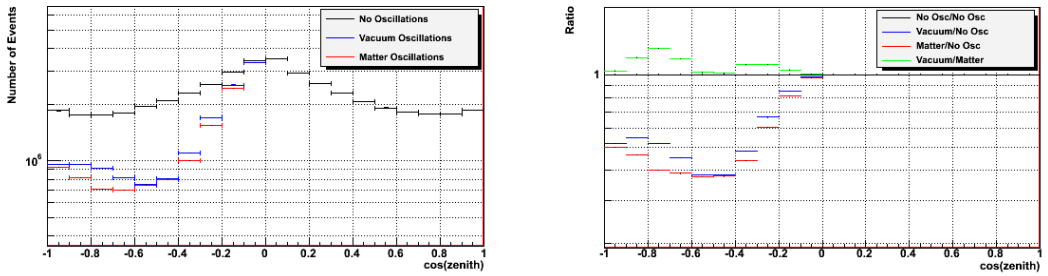

Figure 10: The number of events with zenith angle. The ratio can be seen to drop below one as oscillations become significant, whilst the variation between matter and vacuum is more pronounced.

3.2 Addition of IceCube detector effects

Principally due to its size, the flux of atmospheric neutrino interactions detected by IceCube is far greater than that of many other, smaller neutrino experiments[1]. However, detector effects such as triggering and filtering must now be added to the results in section 3.1. All results presented in this section use Monte Carlo (MC) values.

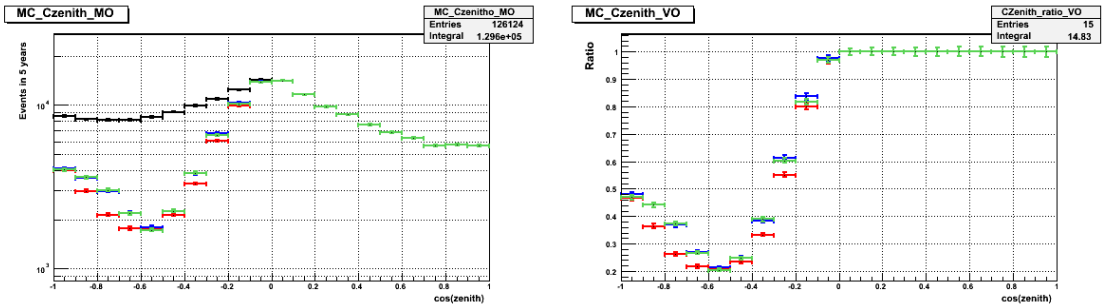

Figure 11: The number of events as a function of zenith angle after triggering and filtering of the detector have been applied. A difference between normal and inverted mass hierarchies is apparent in some bins below $\cos\theta_z = -0.2$. In all plots black corresponds to no oscillations, blue to vacuum oscillations, red to matter oscillations with normal hierarchy and green to matter oscillations with inverted hierarchy.

Figure 11 shows the situation after triggering and filtering of the detector has been applied. The inverted hierarchy case often coincides with the vacuum case; this is due to the resonance (equation (9)) occurring within the parameter space for the normal, but not inverted, mass hierarchy. There is a 10-20% difference between the number of events occurring for normal and inverted mass hierarchies in some bins. However, further cuts are applied to this data as outlined below. As can be seen in figure 12, the deviation in number of events between the cases of normal and inverted mass hierarchies only begins to emerge below approximately 25GeV. This suggests the use of a cut on energies above 25GeV as appropriate to focus into the region of interest in measuring matter effects. Further cuts to the data have been used as follows; firstly the requirement that the first DOM triggered must be within DeepCore. Additionally we require that an interaction is charged current and therefore track producing, whilst to provide a sufficient angular resolution a cut on track-lengths shorter than 20m is made. Finally, for the reconstruction at least 6 DOM hits are required in order to adequately fit the 5 event parameters relating to the direction of origin; x, y, z location, azimuth and zenith angles. Figure 13 shows the number of events after application of the cuts mentioned above as a function of zenith angle. Despite the restrictions, the flux is still about 25 thousand events over five years. The shape of the zenith angle graph in the no oscillation case is unsurprising due to the detector geometry and DOM acceptance.[6]

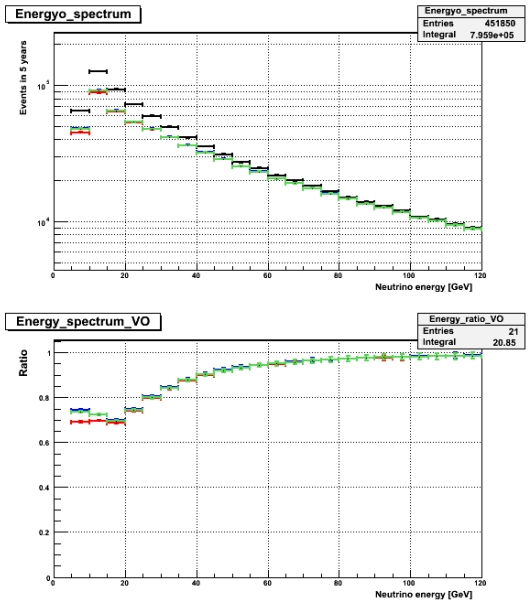

Figure 12: Energy spectrum of combined muon neutrino events prior to application of cuts.

[6]Since all of the DOMs are orientated downwards, upwards travelling muon events are detected (and their direction

Whilst the overall number of events has decreased in figure 13 by the cuts made to figure 11, the shape of the plot remains similar. As is shown in figure 13, after the application of cuts there is still a difference between normal and inverted hierarchy event rates of approximately 10-20% in several bins in the ranges $\cos\theta_z = [-0.9, -0.7]$ and $\cos\theta_z = [-0.4, -0.2]$, which remains to a lesser extent after reconstructions are applied.[7] Provided the data points are not within statistical error of each other, and that the difference is not bridged by systematic errors either, then it may be possible to determine which of the two hierarchy values mostly closely matches an experimental value. For example using the top right plot in figure 13, information from downgoing neutrinos may be used to normalise to the bins in $\cos\theta_z = [-0.6, -0.4]$ at the bottom of the curve, from which a fit to the data may be extended. Comparison of the fit with the expected vacuum value would indicate the hierarchy is normal if below or inverted if in agreement with the vacuum value.

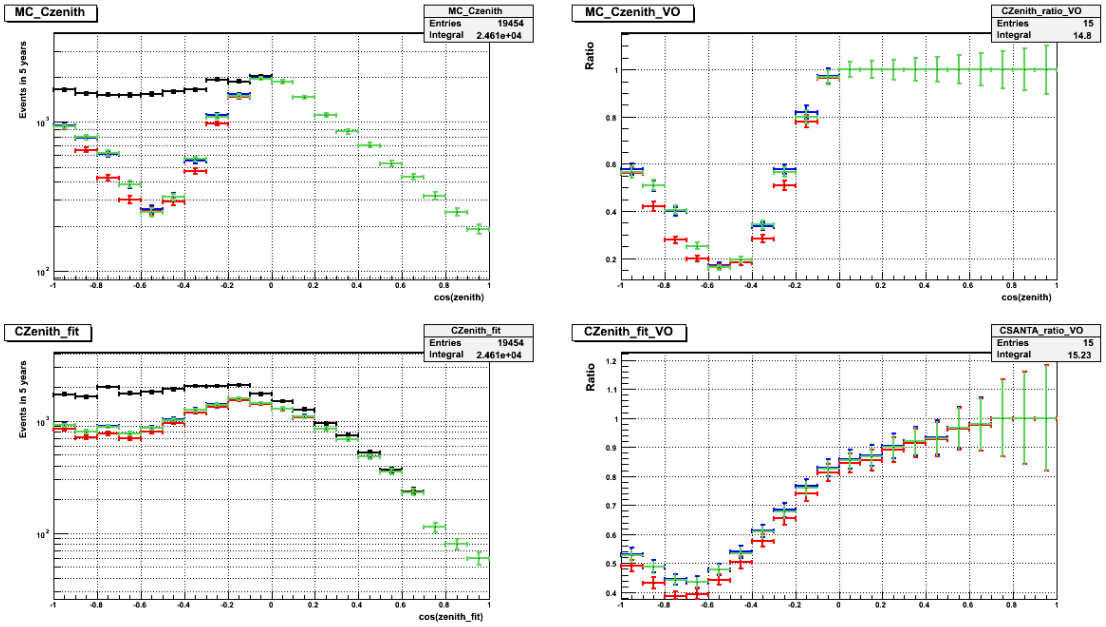

Figure 13: The number of events in 5 years of data collection as a function of zenith angle, top for MC data and bottom after fit reconstruction. There is a clear difference between the values for the two hierarchy schemes in several histogram bins. The errors shown are statistical only.

As a first approach, we naively impose three bins on the bottom right plot in figure 13; the bins from $\cos\theta_z = [-1, -0.3]$, the next 4 and then the remainder. By simply counting events, we obtain a significance of 4.95σ for the first bin, 1.54σ for the second and 0.3σ for the final bin. However, the signal region has been isolated by the cuts on MC values, enhancing the difference, and only statistical errors are included; the effect of systematic errors could easily cause the significance of the first bin to drop below 3σ if not controlled. To help circumvent this, the large region of overlap at higher values of $\cos\theta_z$ may enable the data to be rescaled, reducing some of the effect of systematic errors, but other aspects need further investigation (see section 4). Therefore, five years of data with an accurate reconstruction method may be sufficient to determine experimentally the nature of the mass hierarchy, if systematic errors are mitigated.

reconstructed) with far greater efficiency than those due to downwards travelling muons, the light from which is detected after scattering within the ice.

[7] There is work ongoing in further developing IceCube low energy reconstructions

4 Discussion

In this report, we have presented the theoretical case of matter effects in atmospheric neutrino oscillations due to the Earth, justifying the use of a layered constant density profile. The flavour oscillation probability as a function of both length and energy was calculated and is shown in figures 3 and 4. A realistic neutrino flux was used to produce the plots in section 3.1, whilst addition of IceCube specific detector effects indicated the potential capability of IceCube to determine the neutrino mass hierarchy. For a deviation between normal and inverted hierarchy of that shown in figure 13, the required flux for detection is of the order of 25 thousand events which may be achievable with IceCube in five years. In contrast to new experimental proposals for deducing the nature of the hierarchy (such as Daya Bay [18], T2K [19] or PINGU [20]), which could take 3-4 years to become operational, IceCube is one step ahead in two aspects; it already exists and is already collecting data. This drastically reduces the time-scale for collecting the necessary amount of data. Nevertheless, the difference shown in figure 13 may be rendered undetectable by the presence of systematic errors, such as the efficiency of the DOMs, the rejection of the cosmic ray background, the properties of the ice and the atmospheric neutrino flux. An in depth study of these systematics would be required in order to realise the significance given in section 3.2. Improvements to the reconstruction fit would also enhance the capability of distinguishing between the two cases.

Interesting further lines of investigation could involve introducing a non-zero value of δ_{CP} or changes to the density profile, such as the inclusion of further constant density layers as deemed appropriate, which may affect the difference in effects between normal and inverted hierarchies. The energies at which matter effects are currently detectable with IceCube lie within a narrow region of $\sim 10-25$GeV. Whilst the upper limit on this window is determined by earlier simulation results, as shown in figure 3, the lower limit may be extendible by correcting the flux estimator such that lower energies can be correctly fitted. Figure 13 shows, however, that there is a possibility of the nature of the mass hierarchy becoming detectable by IceCube, if combined with improvements to the fitting algorithms, further effort in understanding the systematic errors and isolating relevant energy range.

Acknowledgements

Many thanks to my supervisors, Rolf Nahnhauer and Juan Pablo Yanez, who had endless patience with answering many questions and dispensing advice. Thanks also to the IceCube group at DESY, for having me join them over the summer and to Karl Jansen, for coordinating both the summer student scheme and the students themselves.

References

[1] Icecube internal wiki pages: `http://wiki.icecube.wisc.edu/index.php/Main_Page` Accessed July - August 2012

[2] E. K. Akhmedov, Phys. Lett. B, **503**, 133 (2001)

[3] T. K. Gaisser, M. Honda, Ann. Rev. Nucl. Part. Sci. **52** 153 (2002)

[4] M. Honda, T. Kajita, K. Kasahara, S. Midorikawa, Phys. Rev. D, **83** 123001 (2011)

[5] C. Giunti, C. W. Kim, *Fundamentals of Neutrino Physics and Astrophysics* (Oxford University Press, New York, 2007)

[6] F. Dufour, D. Wark, `arxiv:1207.3983v1` (2012)

[7] E. K. Akhmedov, V. Niro, JHEP, **12**, 106 (2008)

[8] T. K. Kuo, J. Pantaleone, Phys. Rev. D, **39**, 1930 (1989)

[9] K. Nakamura, S. T. Petcov, Chap. 13 *Neutrino Mass, Mixing and Oscillations* (2010)

[10] A. M. Dziewonski, D. L. Anderson, Phys. Earth Planet. Interiors, **25**, 297 (1981)

[11] T. Ohlsson, H. Snellman, Phys. Lett. B. **474**, 153, (2000)

[12] M. Freund, T. Ohlsson, Mod. Phys. Lett.A **15** 867 (2000)

[13] J. Bernabéu, S. Palomares-Ruiz, A. Pérez, S. T. Percov, Phys. Lett. B **531** 90 (2002)

[14] E. K. Akhmedov, A. Dighe, P. Lipari, A. Y. Smirnov, Nucl. Phys. B **542**, 3 (1999)

[15] C. Andreopoulos et al. Nucl. Instrum. Meth. A **614** 87 (2010)

[16] E. K. Akhmedov, R. Johansson, M. Lindner, T. Ohlsson, T. Schwetz, JHEP, **4**, 78 (2004)

[17] E. K. Akhmedov, M. Maltoni, A. Smirnov, JHEP, **05** 77 (2007)

[18] V. Barger et al., Phys. Rev. Lett., **109** 091801 (2012)

[19] S. Parke, FERMILAB-CONF-06-248-T (2006)

[20] E. K. Akhmedov, S. Razzauq, A. Y. Smirnov, `arXiv:1205.7071v3` (2012)